

See discussions, stats, and author profiles for this publication at: <https://www.researchgate.net/publication/281275587>

Oscillatory Microprocessor for Growth and in Situ Characterization of Semiconductor Nanocrystals

ARTICLE *in* CHEMISTRY OF MATERIALS · AUGUST 2015

Impact Factor: 8.35 · DOI: 10.1021/acs.chemmater.5b02821

READS

43

6 AUTHORS, INCLUDING:



Milad Abolhasani

Massachusetts Institute of Technology

29 PUBLICATIONS 109 CITATIONS

[SEE PROFILE](#)



Ou Chen

Massachusetts Institute of Technology

28 PUBLICATIONS 1,181 CITATIONS

[SEE PROFILE](#)

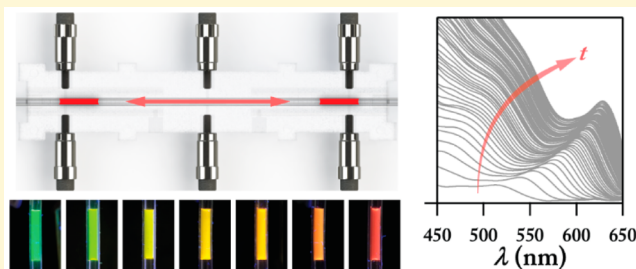
Oscillatory Microprocessor for Growth and in Situ Characterization of Semiconductor Nanocrystals

Milad Abolhasani,[†] Connor W. Coley,[†] Lisi Xie,[†] Ou Chen,[‡] Moungi G. Bawendi,^{*,†} and Klavs F. Jensen^{*,†}

[†]Department of Chemical Engineering and [‡]Department of Chemistry, Massachusetts Institute of Technology, 77 Massachusetts Avenue, 66-342, Cambridge, Massachusetts 02139, United States

Supporting Information

ABSTRACT: An automated two-phase small scale platform based on controlled oscillatory motion of a droplet within a 12 cm long tubular Teflon reactor is designed and developed for high-throughput in situ studies of a solution-phase preparation of semiconductor nanocrystals. The unique oscillatory motion of the droplet within the heated region of the reactor enables temporal single-point spectral characterization of the same nanocrystals with a time resolution of 3 s over the course of the synthesis time without sampling while removing the residence time limitation associated with continuous flow-based strategies. The developed oscillatory microprocessor allows for direct comparison of the high temperature and room temperature spectral characteristics of nanocrystals. Utilizing this automated experimental strategy, we study the effect of temperature on the nucleation and growth of II–VI and III–V semiconductor nanocrystals. The automated droplet preparation and injection of the precursors combined with the oscillatory flow technique allows 7500 spectral data within a parameter space of 10 min reaction time at ten different temperatures and five different precursor ratios to be obtained automatically using only 250 μ L of each precursor solution. The oscillatory microprocessor platform provides real-time in situ spectral information at the synthesis temperature, vital for fundamental studies of different mechanisms involved during the nucleation and growth stages of different types of nanomaterials.



The emergence of semiconductor nanocrystals, known as quantum dots (QDs), with unique physicochemical properties have enabled breakthrough applications at cellular and organism scales in biological imaging^{1–7} and at device scales in light emitting diodes,^{8–12} solar cells,^{13–15} and displays.^{16,17} Owing to the quantized energy levels associated with nanometer-sized QDs, their corresponding absorption and photoluminescence emission spectra are directly correlated and tuned with the size of QDs. The batch scale process for the solution-phase preparation of QDs (Figure 1a) that was introduced ~20 years ago¹⁸ still remains as the primary method for screening, exploration, and investigation of new classes of nanomaterials. The lack of control over the experimental parameters and unavailability of spectral information during intermediate growth stages of nanocrystals have inhibited the development and optimization of III–V QDs. Moreover, the manual nature of batch scale techniques makes high-throughput screening and fundamental studies of colloidal QDs both time- and labor-intensive.

Reducing the reaction vessel size from liters to microliters significantly enhances the heat and mass transfer rates during the synthesis process of QDs while enabling precise control over the reaction parameters. Over the past 15 years, different single/multiphase microscale strategies have demonstrated promising flow-based alternatives to batch scale syntheses for

screening of a large parameter space associated with nanomaterial synthesis.^{19–37} Recently, deMello et al.³⁸ developed a continuous flow strategy for in-flow studies of IV–VI QDs (PbS) and reported kinetics of lead sulfide nanocrystals during nucleation and growth stages. However, the constant length of the microreactor, L , shown in Figure 1b, and intrinsic dependence of the degree of mixing on residence times (via average flow velocity) associated with continuous microscale platforms make it challenging to reproduce the same mixing characteristics for different synthesis times.^{39–41} In addition, most microscale strategies still require approximately milliliter volumes of QD precursors for each experimental condition (e.g., concentration and reaction time) due to the dead volume associated with tubing and waiting time required to reach steady state conditions after changing flow parameters.

For this work, building on a recently developed oscillatory flow reactor technique,^{39,42,53} we designed and developed an integrated, modular flow-based strategy for in situ characterization and fundamental studies of the synthesis of colloidal semiconductor nanocrystals. As a proof of concept, we first use our oscillatory microprocessor for screening of the well-studied

Received: July 22, 2015

Revised: August 12, 2015

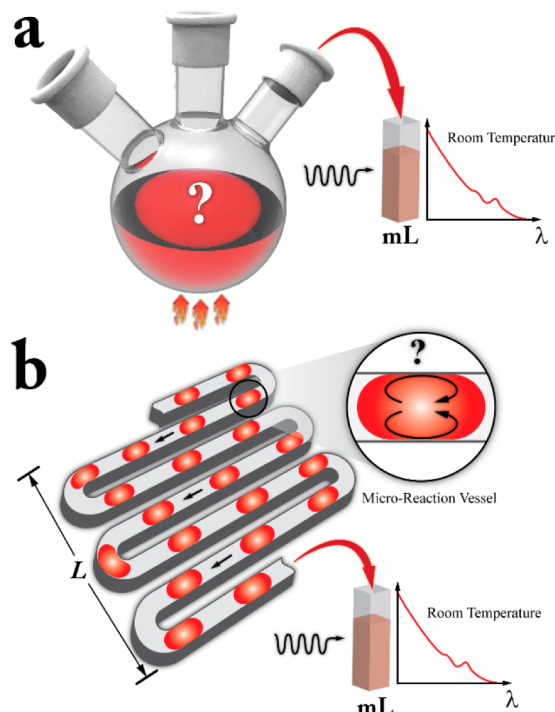


Figure 1. Schematic of (a) batch (hot-injection) and (b) continuous flow reactor (droplet-based) strategies for screening and characterization of colloidal nanomaterials. The inset in (b) shows one of a few hundred microreaction vessels that are formed in flow for each reaction condition.

II–VI QDs (i.e., CdSe and CdTe) and demonstrate the information that can be obtained using integrated *in situ* spectroscopy during the nucleation and growth stages of QDs.

In the next step, we apply our two-phase strategy to studies of III–V QDs (i.e., InP) and report the high temperature *in situ* spectral evolution of these semiconductor nanocrystals during the nucleation and growth stages within the same droplet and without the need for setup manipulation. The automated delivery and injection of the precursors enables a robust and reproducible synthesis procedure, thereby enabling fundamental studies of the nucleation and growth kinetics of the semiconductor nanocrystals. The two-phase oscillatory platform enables time- and cost-efficient screening and optimization of semiconductor nanocrystals over a wide spectral range (300–1900 nm) and could potentially be applied for characterization and studies of other types of nanomaterials.

EXPERIMENTAL SECTION

Oscillatory Microprocessor. The automated oscillatory microprocessor, shown in Figure 2, consists of a 12 cm long Teflon tubular reactor (0.0625 in. inner diameter, fluorinated ethylene propylene (FEP)) embedded within a custom-machined aluminum chuck, two fiber-coupled LEDs, and photodetectors, as well as a fiber-coupled UV-vis light source and a miniature spectrometer. Four cartridge heaters embedded within the aluminum chuck (two on each side) in combination with a thermocouple embedded in the aluminum chuck are used for heating the reactor (see Supporting Information Figure S7). Three computer-controlled syringe pumps are used to prepare the droplet with the desired molar ratio under inert atmosphere (argon) and control its oscillation within the heated zone of the reactor. First, a 5–10 μ L droplet containing precursor I is formed at the first T-junction and is then automatically moved toward the second T-junction using syringe 1 (pressurized argon, 10 psig). In the next step, using the tube volume between the two T-junctions, the second

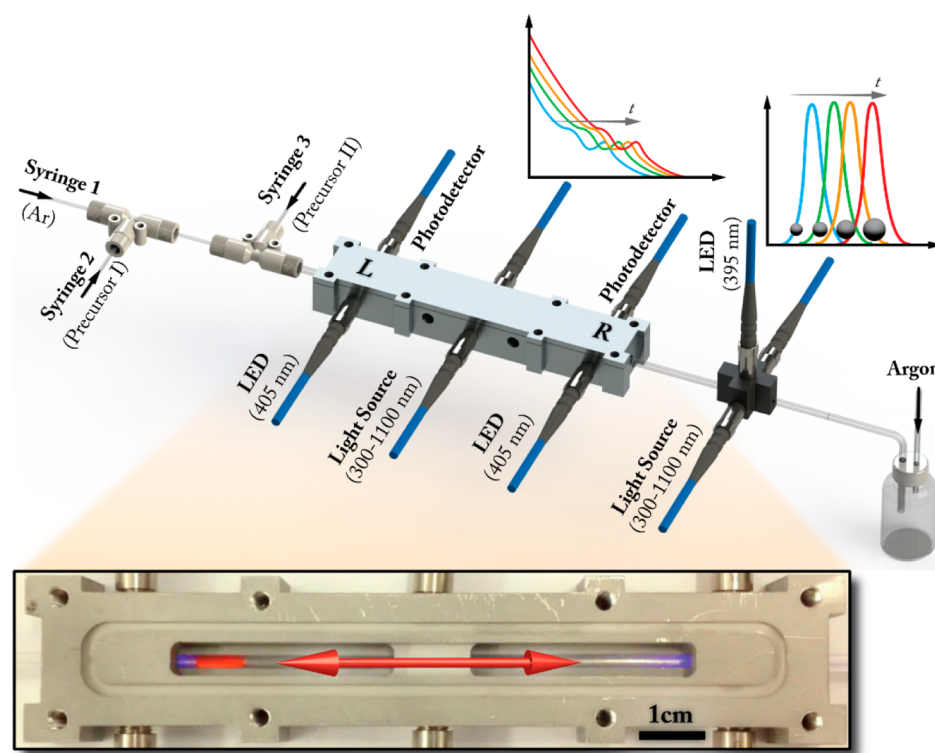


Figure 2. (a) Schematic of the oscillatory microprocessor. The inset shows an image of a droplet oscillating inside the tubular FEP reactor embedded within the aluminum chuck (see Movie M1 for the oscillatory motion of a droplet within the FEP reactor). Carrier phase is argon (10 psig).

precursor ($5\text{--}10 \mu\text{L}$) is automatically injected into the droplet of precursor I at the second T-junction. The prepared droplet is then moved into the heated zone ($160\text{--}220^\circ\text{C}$) of the reactor using syringe 1 and oscillated back and forth between the two integrated fibers located at each end of the reactor for the predefined reaction time and a set flow velocity (Figure 3a). The change in the measured

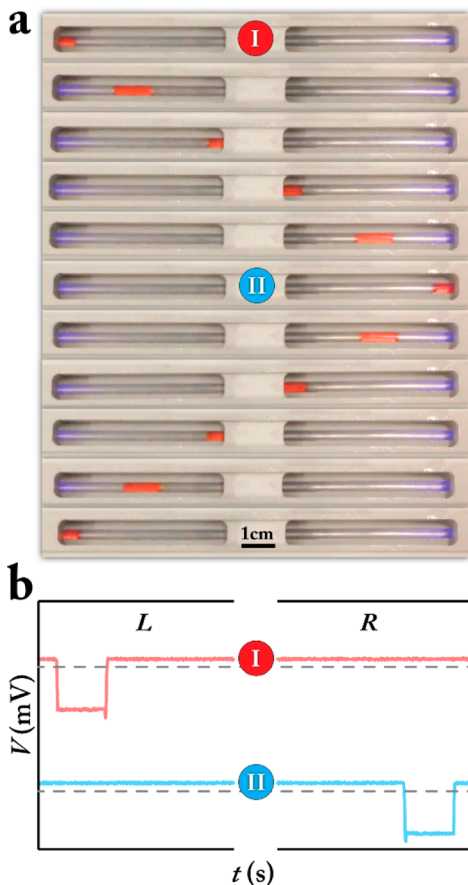


Figure 3. (a) Time-series of bright-field images of one complete oscillation cycle of a droplet within the FEP reactor. (b) Measured voltages of the two photodetectors placed on the left, *L*, and right, *R*, sides of the aluminum chuck at times (I) and (II) highlighted in (a). The dashed gray line shows the threshold voltage used for switching the flow direction of the carrier syringe.

voltage of the photodetectors, shown in Figure 3b, is used as a threshold criterion to automatically switch the flow direction of syringe 1 (using LabVIEW), and thereby oscillate the droplet within the heated zone of the reactor. The overall process flow, including the droplet formation, injection of precursor II into the previously formed droplet of precursor I, and *in situ* absorption spectra data acquisition, was computer-controlled via two LabVIEW scripts (see Figure S1 for more details of the experimental setup). The constant oscillatory motion ensures well-stirred mixing inside the droplet owing to the two recirculation zones formed inside the droplet as in traditional segmented flow (inset of Figure 1b). It has previously been demonstrated that the stirring strength within the two recirculation zones formed inside a droplet containing two miscible fluids flowing along the flow direction is directly correlated with the flow velocity.^{43,44} Thus, adjusting the flow velocity to achieve different residence times would result in different mixing characteristics for the two miscible fluids inside a droplet flowing along the flow direction.

The automated oscillatory motion of the droplet within the reactor removes the three major limitations of continuous multiphase platforms, (a) inter-relation of mixing characteristics and residence time, (b) residence time limitation due to a constant tube length, and

(c) lack of *in situ* characterization of individual droplets for multiple residence times. In contrast to continuous multiphase strategies, the oscillatory microprocessor allows utilization of the same flow velocity, U_0 , thereby providing the same degree of mixing for different growth times and enabling single-point measurement of the same micro-reaction vessel without the need to adjust the flow velocity or the reactor length. Increasing the flow velocity or decreasing the reactor length will linearly decrease the time required for the droplet to complete each path inside the oscillatory zone, thereby decreasing the time-delay between each absorption measurement. However, as previously demonstrated by Thulasidas et al.,⁴⁵ the minimum required travel distance for a liquid droplet to form a complete recirculation (stirring) is three times the total length of the liquid droplet (i.e., a minimum reactor length of $\sim 3 \text{ cm}$ for a $20 \mu\text{L}$ droplet). Taking into account the minimum travel length of a droplet, as well as the time required for switching of the flow direction of the carrier syringe pump (syringe 1 in Figure 2) at each end of the oscillatory zone, and the time required for the droplet to reach a constant velocity, we selected a total oscillatory flow reactor length of 12 cm from the left to the right side fiber-coupled LEDs to cover a wide range of droplet volumes ($5\text{--}30 \mu\text{L}$). Moreover, utilization of an inert gas (argon) as the carrier phase removes the need for finding a solvent with negligible miscibility with the QD solvent (octadecene) at high temperatures. The integration of the two-phase oscillatory platform with spectral characterization tools (i.e., absorption and fluorescence spectroscopy) enables real-time *in situ* monitoring of the in-flow prepared QDs with a time resolution of 3 s, which is otherwise impossible to accomplish in batch scale synthesis (limited to tens of seconds). A custom-machined flow-cell located downstream of the reactor is used for direct comparison of the high temperature to room temperature absorbance of the same semiconductor nanocrystals. Moreover, a third fiber port (perpendicular to the miniature spectrometer fiber) within the same flow-cell enables *in-line* photoluminescence, PL, measurements of the in-flow prepared QDs.

Chemicals. Cadmium oxide (CdO , 99.99% trace metals basis), selenium (Se, 99.5% trace metals basis), tellurium (Te, 99.8% trace metals basis), 1-octadecene (ODE, technical grade, 90%), oleic acid (OA, technical grade, 90%), oleylamine (OLA, technical grade, 70%), myristic acid (MA, >99%), and hexane (laboratory reagent, 95%) were purchased from Sigma-Aldrich. Indium acetate ($\text{In}(\text{Ac})_3$, 99.99% metals basis) was purchased from Alfa Aesar. Trioctylphosphine (TOP, min, 90%) and tris(trimethylsilyl)phosphine ($\text{P}(\text{TMS})_3$) were purchased from Strem Chemicals.

Precursor Preparations. Cd Precursor (10 mM). To a 250 mL round-bottom flask were added 130 mg of CdO , 6.4 mL of oleic acid, and 93.6 mL of ODE. The mixture was degassed under vacuum for 1 h at room temperature, and then degassed under vacuum at 110°C for another 1 h. The solution mixture was then heated in an oil bath under argon atmosphere at 190°C until the mixture clarified to become a colorless solution ($\sim 30 \text{ min}$). The solution was then allowed to cool to room temperature before use.

Se Precursor (20 mM). Ninety-one milliliters of ODE was degassed under vacuum for the preparation of Se precursors. First, 160 mg of Se powder and 9 mL of TOP were mixed in a glovebox and stirred overnight to become a colorless solution. The TOP-Se mixture was then added to 91 mL of degassed ODE in a round-bottom flask under inert atmosphere.

Te Precursor (20 mM). Te (38.3 mg) was mixed with 13.6 mL of degassed ODE and 1.4 mL of TOP. The mixture was stirred until the solution became clear.

In Precursor (40 mM). First, indium myristate was synthesized from $\text{In}(\text{Ac})_3$. In a Schlenk line, 10 mmol $\text{In}(\text{Ac})_3$ (2.93 g) and 30 mmol MA (7.00 g) were mixed in 15 mL of ODE. The mixture was then heated to 120°C under vacuum for 2.5 h to form a clear solution. The solution was then cooled to room temperature under inert atmosphere, where white solids precipitated. The precipitated solid was washed 4 times with hexane, vacuum-dried overnight, and then stored in a glovebox. In the next step, 159.4 mg of indium myristate was mixed with 0.2 mL of TOP, 0.2 mL of degassed OLA (only for the case with amine), and 4.6 mL of degassed ODE. The solution was then

heated to 80 °C to become colorless and was used after cooling to room temperature.

Precursor (20 mM). P(TMS)₃ (100 mg) was mixed with 20 mL of degassed ODE under inert atmosphere.

RESULTS AND DISCUSSION

Characterization of II–VI QDs. Utilizing the developed oscillatory microprocessor, we first studied the nucleation and growth stages of II–VI (CdSe and CdTe) QDs at different reaction temperatures (160–220 °C) and growth times (3–900 s) via the in situ obtained absorption spectra of the prepared QDs using only 5 μL of each QD precursor solution.

Figure 4a shows the in situ absorption spectra evolution of a 10 μL droplet containing CdSe nanocrystals with a time delay of 4 s at 220 °C and Cd:Se molar ratio of 1:2. A custom-developed MATLAB script was implemented within the LabVIEW program for real-time extraction of the first

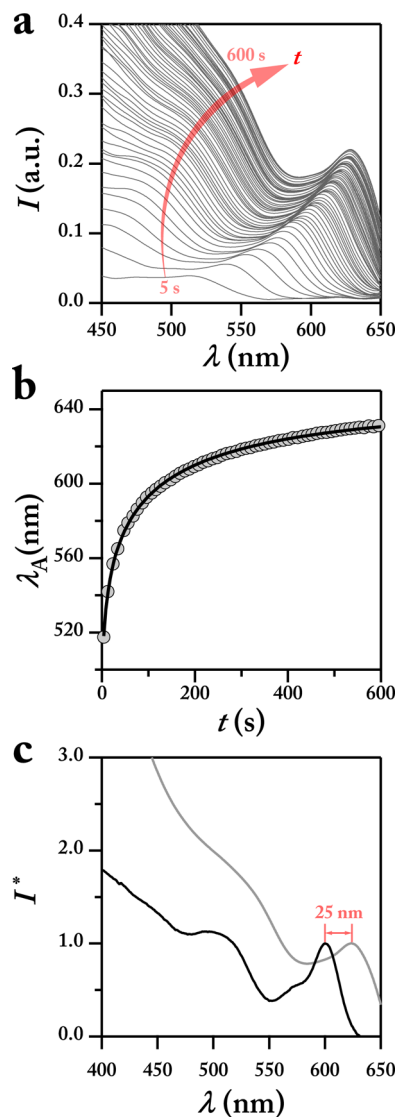


Figure 4. In situ time evolution of (a) absorption spectra (b) and first absorption peak of CdSe QDs at $T = 220\text{ }^{\circ}\text{C}$, Cd:Se 1:2 molar ratio, $U_0 = 4\text{ cm/s}$, and Cd: 5 μL (precursor I) and Se: 5 μL (precursor II). Integration time of 20 ms was used for each absorption spectrum. (c) In situ comparison of absorption spectrum of the same CdSe QDs at $T = 23\text{ }^{\circ}\text{C}$ (gray) and $T = 220\text{ }^{\circ}\text{C}$ (black).

absorption peak wavelength of the in-flow synthesized QDs. Figure 4b shows the time evolution of the first absorption peak of the same CdSe QDs over the course of a 10 min reaction time.

Figure 4c shows the direct comparison of the absorption spectra of the same CdSe QDs at 220 and 23 °C (see Figure S8 for more room temperature absorption spectra of CdSe QDs). As shown in this figure, in comparison to the room temperature data, there is a red-shift of 25 nm for the UV-vis absorption spectrum of CdSe QDs at the synthesis temperature.⁴⁶ In addition, the half-width-at-half-maximum (HWHM) of the first absorption peak of CdSe QDs at the synthesis temperature (220 °C) is ~33% broader than at room temperature (23 °C) for the same synthesis time (and the same nanocrystals) due to the occurrence of thermal broadening.^{46,47}

Figure 5 shows the PL characterization of in-flow synthesized CdSe QDs. The time evolution of PL spectra of CdSe QDs at 220 °C is shown in Figure 5a. As shown in Figure 5a and b, the continuous formation of CdSe QDs at the early stages of the synthesis process results in an asymmetric PL spectrum with a relatively large full-width-at-half-maximum (fwhm). In the next growth stage of the CdSe QDs, the smaller nanocrystals start to grow faster than the larger QD nanocrystals, resulting in the size distribution focusing of CdSe QDs as evidenced by the narrow fwhm of 28 nm at 485 s of residence time (Figure 5b). Following this stage, Ostwald ripening takes over, resulting in the disappearance of the smaller and growth of the larger nanocrystals and increase of the fwhm (i.e., size distribution) of the semiconductor nanocrystals. A transmission electron microscopy (TEM) image of as-prepared CdSe QDs at 220 °C is shown in Figures 5d. The narrow size distribution of CdSe QDs shown in Figure 5d further demonstrates the capability of the oscillatory microprocessor for in-flow screening and characterization of high quality QDs.

In the next step, we applied the oscillatory microprocessor for in situ studies of the effect of temperature on the growth rate of CdSe QDs. Figure 6a shows in situ absorption spectra of CdSe QDs at different temperatures with the same Cd:Se molar ratio of 1:2 acquired with automated preparation and injection of a 10 μL droplet for each synthesis temperature. The oscillatory microprocessor enables automated data acquisition and processing of 60–150 absorption spectra over the course of the QD synthesis without the need for any sampling or manual processing while using only 5 μL of each precursor solution.

Figure 6b shows the kinetics of CdSe QD growth through time evolution of the first excitonic absorption peak wavelength, λ_A , of CdSe QDs at temperatures ranging between 160 and 220 °C using a total of 60 μL of Cd and Se precursors. As can be seen in Figure 6b, increasing temperature from 160 to 200 °C significantly accelerates growth of CdSe QDs; however, this effect is less dramatic from 200 to 220 °C. The enhanced growth and higher quality of CdSe QDs at higher temperatures can be attributed to the faster nucleation (i.e., higher degree of supersaturation to overcome the nucleation energy barrier) at higher temperatures, resulting in a faster decrease of monomer concentrations below supersaturation (homogeneous formation of nanocrystal nuclei), thereby inhibiting further nucleation formation, whereas temperatures below 200 °C, the lower degree of supersaturation, result in the continuous formation of nanocrystal nuclei.⁴⁸ The continuous formation of nanocrystal nuclei at lower temperatures (i.e., lower degree of supersaturation) results in combined growth and nuclei formation of nanocrystals, thereby widening the first excitonic absorption

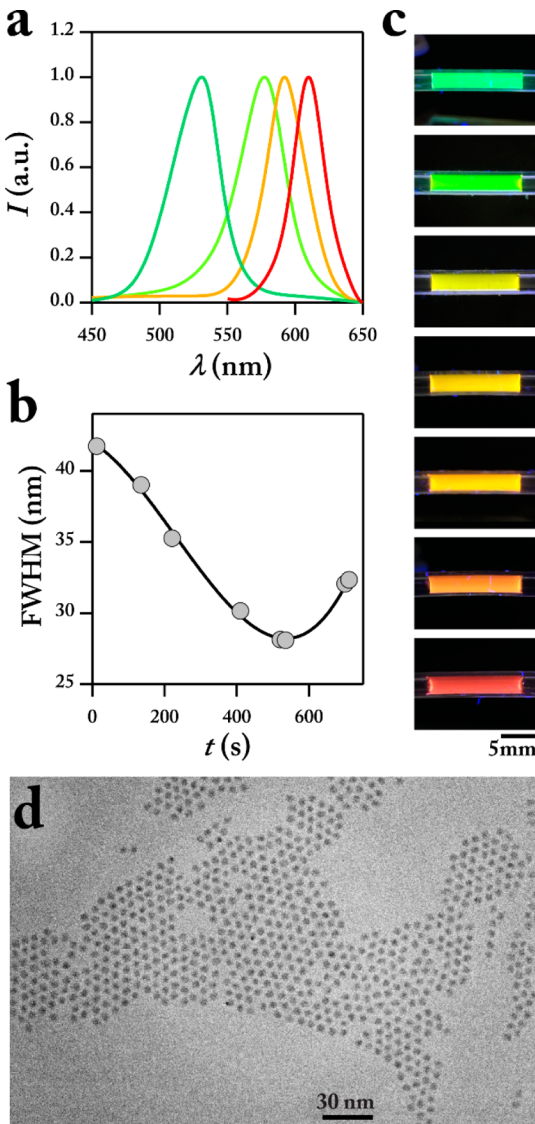


Figure 5. In situ screening of (a) photoluminescence and (b) time evolution of fwhm of CdSe QDs synthesized at $T = 220\text{ }^{\circ}\text{C}$, $U_0 = 1\text{ cm/s}$, Cd:Se 1:2 molar ratio and $t = 12\text{ s}$ (dark green), 135 s (light green), 231 s (orange), and 535 s (red); Cd: $5\text{ }\mu\text{L}$ (precursor I) and Se: $5\text{ }\mu\text{L}$ (precursor II). An integration time of 1 s and excitation wavelength of 395 nm were used for all PL spectra. (c) Fluorescence images of a $20\text{ }\mu\text{L}$ droplet containing the same QDs taken at different growth times. (d) TEM image of CdSe QDs with an average size of $4 \pm 0.23\text{ nm}$, synthesized at $T = 220\text{ }^{\circ}\text{C}$, Cd:Se 1:2 molar ratio, $U_0 = 1\text{ cm/s}$ and $t = 152\text{ s}$; Cd: $5\text{ }\mu\text{L}$ (precursor I) and Se: $5\text{ }\mu\text{L}$ (precursor II).

spectra of QDs (larger size distribution) and smaller nanocrystals for the same synthesis time and Cd:Se molar ratios.

Utilizing the two-phase oscillatory microprocessor platform, we also studied the effect of temperature on the kinetics of growth of another II–VI QD (i.e., CdTe). Figure 7a shows the time evolution of the absorption spectra of CdTe QDs at $160\text{ }^{\circ}\text{C}$. Similar to CdSe QDs, increasing the temperature from 160 to $180\text{ }^{\circ}\text{C}$ significantly enhances the growth rate of CdTe QDs (shown in Figure 7b).

Characterization of III–V QDs. To demonstrate the versatility of the developed two-phase strategy, as the final case study, we utilized the oscillatory microprocessor platform for in situ screening of III–V QDs (InP) with and without the

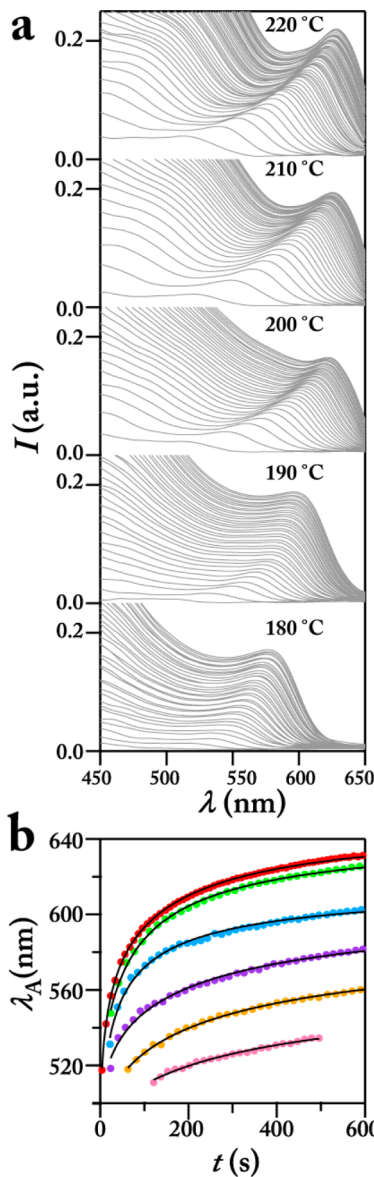


Figure 6. (a) In situ time evolution of absorption spectra of CdSe QDs at different growth temperatures. (b) In situ time evolution of the first absorption peak wavelength of CdSe QDs shown in (a) at growth temperatures of $160\text{ }^{\circ}\text{C}$ (pink), $170\text{ }^{\circ}\text{C}$ (orange), $180\text{ }^{\circ}\text{C}$ (purple), $190\text{ }^{\circ}\text{C}$ (blue), $200\text{ }^{\circ}\text{C}$ (green), and $220\text{ }^{\circ}\text{C}$ (red). Cd: $5\text{ }\mu\text{L}$ (precursor I) and Se: $5\text{ }\mu\text{L}$ (precursor II). Integration time of 20 ms was used for each absorption spectrum.

presence of amines (oleylamine). Panels a and b in Figure 8 show a time-series of in situ absorption spectra of InP QDs without amine at $220\text{ }^{\circ}\text{C}$. The time evolution of the first absorption peak wavelength of the in-flow synthesized InP QDs is shown in Figure 8c. The red-shift and broadening of the first excitonic absorption peak of InP QDs may suggest that the growth of InP nanocrystals is mostly governed by ripening and intermolecular interactions, as previously proposed by Harris et al.⁴⁹ The intermediate growth mechanism of III–V QDs suggests that the absence of a size focusing stage during the growth period of InP QDs (in contrast with II–VI QDs) due to the depletion of the precursors throughout the formation of nanocrystal nuclei is one of the key factors contributing to inhomogeneous broadening of the resulting III–V QDs.^{50,51} Figure 8d shows the in situ absorption spectra evolution of InP

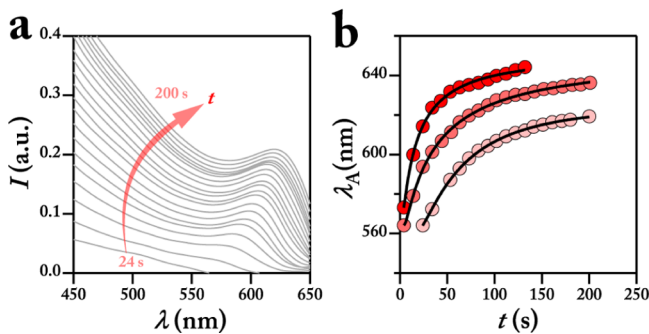


Figure 7. (a) In situ absorption spectra evolution of CdTe QDs at a Cd:Te molar ratio of 1:2, growth temperature of 160 °C, and $U_0 = 1$ cm/s. (b) Time evolution of first absorption peak wavelength of CdTe QDs with Cd:Te 1:2 molar ratio and $T = 160$ °C (light pink), 170 °C (dark pink), and 180 °C (red). Cd: 5 μ L (precursor I) and Te: 5 μ L (precursor II). Integration time of 20 ms was used for each absorption spectrum.

QDs in the presence of amine (oleylamine) at temperatures of 180 and 220 °C.

As can be seen in Figure 8d, the nucleation and growth stages of InP QDs occur at a time scale below 10 s (the black line is the first acquired absorption spectrum after 4 s). Then, ripening of nonmolecular InP causes inhomogeneous broadening of the resulting nanocrystals similar to the case without amine. As can be seen in Figure 8, the presence of amine has increased the rate of nucleation of InP QDs, resulting in a faster depletion of the precursors and smaller sized nanocrystals with a final λ_A of 490 nm compared to the same case without amine (530 nm).⁵² Figure 8e shows the direct comparison of the high temperature to room temperature absorption spectra of in-flow prepared InP QDs (see Figure S10 for a TEM image of InP QDs). As can be seen in Figure 8e, the red-shift of the high temperature absorption spectra decreases from 33 nm at 220 °C to 17 nm at 180 °C.

CONCLUSIONS

In conclusion, we designed and developed the first fully automated small-scale strategy for in situ studies of the solution-phase synthesis of semiconductor nanocrystals. The controlled oscillatory motion of the droplets within the Teflon reactor provided similar mixing characteristics for different reaction times and removed the residence time limitation associated with continuous multiphase strategies. A time-series of absorption spectra with a time delay of 3–15 s was obtained at each reaction temperature from a single 10 μ L droplet containing the QD nanocrystals while moving back and forth within a 12 cm long reactor with an average velocity of 1–4 cm/s. To the best of our knowledge, our developed experimental platform is the first small-scale strategy that enables in situ spectral characterization of II–VI and III–V QDs at the synthesis temperature, providing further insights into the kinetics and mechanisms of nucleation and growth stages of colloidal nanocrystals without the need for sampling or setup manipulation. The oscillatory microprocessor could further be applied toward high-throughput in situ screening and optimization of other classes of QDs (e.g., near IR) with different objective functions (e.g., quantum yield and nanocrystal size and distribution) for applications in (nontoxic) bioimaging and cadmium-free QD displays. Moreover, owing to the independence of the mixing and residence times, the

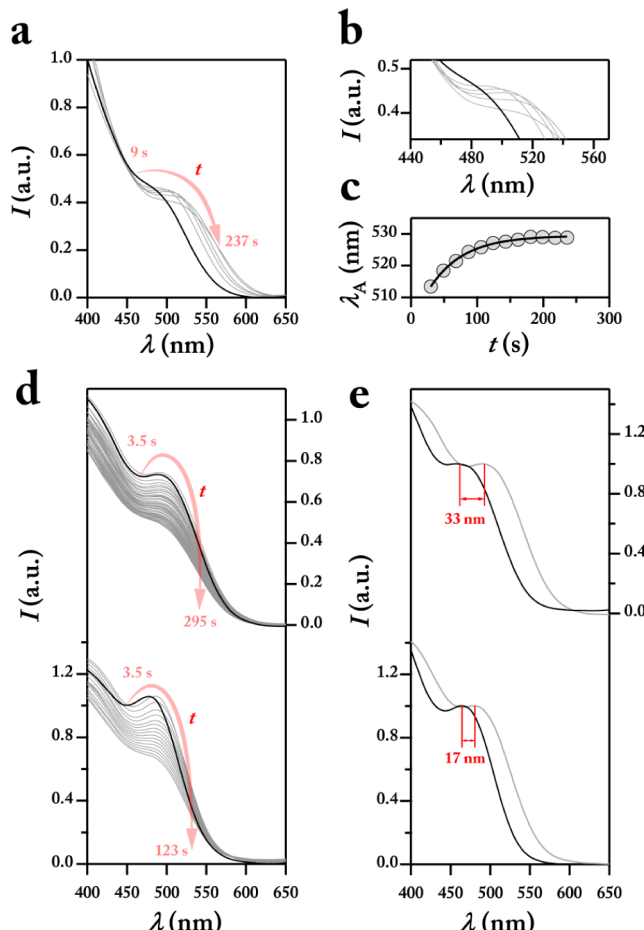


Figure 8. (a) In situ absorption spectra evolution of InP QDs without the presence of OLA in In precursor; In:P 2:1, $T = 220$ °C, $U_0 = 1$ cm/s. In: 5 μ L (precursor I) and P: 5 μ L (precursor II). (b) Enlarged view of the absorption spectra evolution of InP QDs shown in (a). (c) Time evolution of the first absorption peak wavelength of InP QDs shown in (a). (d) In situ absorption spectra evolution of InP QDs with the presence of OLA in the In precursor, In:P molar ratio of 2:1, growth temperature of (top) 220 °C and (bottom) 180 °C, and $U_0 = 2$ cm/s. In: 5 μ L (precursor I) and P: 5 μ L (precursor II). (e) Direct in situ comparison of absorption spectrum of the same InP QDs at $T = 23$ °C (gray) and the growth temperature (black). (top) $T = 220$ °C, $t = 14$ s and (bottom) $T = 180$ °C, $t = 42$ s. Integration time of 20 ms was used for each absorption spectrum.

oscillatory microprocessor could potentially be applied toward studies of multistage nanomaterial synthesis, such as core/shell QDs, without the need for hardwiring long (>5 m) tubular reactors in series. Finally, the optimized synthesis conditions obtained with the oscillatory microprocessor could directly be transferred to continuous scaled-up nanomanufacturing of semiconductor nanocrystals with similar characteristic length scales.

ASSOCIATED CONTENT

S Supporting Information

The Supporting Information is available free of charge on the ACS Publications website at DOI: 10.1021/acs.chemmater.5b02821.

Details of the experimental setup and the automated oscillatory motion (PDF)

Video demonstrating the oscillatory motion of a droplet within the FEP reactor ([AVI](#))

AUTHOR INFORMATION

Corresponding Authors

*E-mail: mgb@mit.edu.

*E-mail: kfjensen@mit.edu. Homepage: <http://web.mit.edu/jensenlab>.

Notes

The authors declare no competing financial interest.

ACKNOWLEDGMENTS

This work was supported by National Science Foundation (NSF) Grant ECCS-1449291. M.A. gratefully acknowledges financial support from an NSERC Postdoctoral Fellowship. C.W.C. thanks the NSF Graduate Research Fellowship Program for Grant 1122374.

REFERENCES

- (1) Medintz, I. L.; Uyeda, H. T.; Goldman, E. R.; Mattoussi, H. Quantum dot bioconjugates for imaging, labelling and sensing. *Nat. Mater.* **2005**, *4*, 435–446.
- (2) Michalet, X.; Pinaud, F. F.; Bentolila, L. A.; Tsay, J. M.; Doose, S.; Li, J. J.; Sundaresan, G.; Wu, A. M.; Gambhir, S. S.; Weiss, S. Quantum Dots for Live Cells, in Vivo Imaging, and Diagnostics. *Science* **2005**, *307*, 538–544.
- (3) Chan, W. C. W.; Nie, S. Quantum Dot Bioconjugates for Ultrasensitive Nonisotopic Detection. *Science* **1998**, *281*, 2016–2018.
- (4) Soo Choi, H.; Liu, W.; Misra, P.; Tanaka, E.; Zimmer, J. P.; Itty Ipe, B.; Bawendi, M. G.; Frangioni, J. V. Renal clearance of quantum dots. *Nat. Biotechnol.* **2007**, *25*, 1165–1170.
- (5) Wong, C.; Stylianopoulos, T.; Cui, J.; Martin, J.; Chauhan, V. P.; Jiang, W.; Popović, Z.; Jain, R. K.; Bawendi, M. G.; Fukumura, D. Multistage nanoparticle delivery system for deep penetration into tumor tissue. *Proc. Natl. Acad. Sci. U. S. A.* **2011**, *108*, 2426–2431.
- (6) Chauhan, V. P.; Stylianopoulos, T.; Martin, J. D.; Popovic, Z.; Chen, O.; Kamoun, W. S.; Bawendi, M. G.; Fukumura, D.; Jain, R. K. Normalization of tumour blood vessels improves the delivery of nanomedicines in a size-dependent manner. *Nat. Nanotechnol.* **2012**, *7*, 383–388.
- (7) Chen, O.; Zhao, J.; Chauhan, V. P.; Cui, J.; Wong, C.; Harris, D. K.; Wei, H.; Han, H.-S.; Fukumura, D.; Jain, R. K.; Bawendi, M. G. Compact high-quality CdSe–CdS core–shell nanocrystals with narrow emission linewidths and suppressed blinking. *Nat. Mater.* **2013**, *12*, 445–451.
- (8) Sun, Q.; Wang, Y. A.; Li, L. S.; Wang, D.; Zhu, T.; Xu, J.; Yang, C.; Li, Y. Bright, multicoloured light-emitting diodes based on quantum dots. *Nat. Photonics* **2007**, *1*, 717–722.
- (9) Caruge, J. M.; Halpert, J. E.; Wood, V.; Bulovic, V.; Bawendi, M. G. Colloidal quantum-dot light-emitting diodes with metal-oxide charge transport layers. *Nat. Photonics* **2008**, *2*, 247–250.
- (10) Coe, S.; Woo, W.-K.; Bawendi, M.; Bulovic, V. Electroluminescence from single monolayers of nanocrystals in molecular organic devices. *Nature* **2002**, *420*, 800–803.
- (11) Mashford, B. S.; Stevenson, M.; Popovic, Z.; Hamilton, C.; Zhou, Z.; Breen, C.; Steckel, J.; Bulovic, V.; Bawendi, M.; Coe-Sullivan, S.; Kazlas, P. T. High-efficiency quantum-dot light-emitting devices with enhanced charge injection. *Nat. Photonics* **2013**, *7*, 407–412.
- (12) Shirasaki, Y.; Supran, G. J.; Bawendi, M. G.; Bulovic, V. Emergence of colloidal quantum-dot light-emitting technologies. *Nat. Photonics* **2012**, *7*, 13–23.
- (13) Kongkanand, A.; Tvrdy, K.; Takechi, K.; Kuno, M.; Kamat, P. V. Quantum Dot Solar Cells. Tuning Photoresponse through Size and Shape Control of CdSe–TiO₂ Architecture. *J. Am. Chem. Soc.* **2008**, *130*, 4007–4015.
- (14) Sargent, E. H. Colloidal quantum dot solar cells. *Nat. Photonics* **2012**, *6*, 133–135.
- (15) Chuang, C.-H. M.; Brown, P. R.; Bulović, V.; Bawendi, M. G. Improved performance and stability in quantum dot solar cells through band alignment engineering. *Nat. Mater.* **2014**, *13*, 796–801.
- (16) Kim, T.-H.; Cho, K.-S.; Lee, E. K.; Lee, S. J.; Chae, J.; Kim, J. W.; Kim, D. H.; Kwon, J.-Y.; Amarantunga, G.; Lee, S. Y.; Choi, B. L.; Kuk, Y.; Kim, J. M.; Kim, K. Full-colour quantum dot displays fabricated by transfer printing. *Nat. Photonics* **2011**, *5*, 176–182.
- (17) Lee, J.; Sundar, V. C.; Heine, J. R.; Bawendi, M. G.; Jensen, K. F. Full Color Emission from II–VI Semiconductor Quantum Dot–Polymer Composites. *Adv. Mater.* **2000**, *12*, 1102–1105.
- (18) Murray, C. B.; Norris, D. J.; Bawendi, M. G. Synthesis and characterization of nearly monodisperse CdE (E = sulfur, selenium, tellurium) semiconductor nanocrystallites. *J. Am. Chem. Soc.* **1993**, *115*, 8706–8715.
- (19) Yen, B. K. H.; Günther, A.; Schmidt, M. A.; Jensen, K. F.; Bawendi, M. G. A Microfabricated Gas–Liquid Segmented Flow Reactor for High-Temperature Synthesis: The Case of CdSe Quantum Dots. *Angew. Chem.* **2005**, *117*, 5583–5587.
- (20) Baek, J.; Allen, P. M.; Bawendi, M. G.; Jensen, K. F. Investigation of Indium Phosphide Nanocrystal Synthesis Using a High-Temperature and High-Pressure Continuous Flow Microreactor. *Angew. Chem.* **2011**, *123*, 653–656.
- (21) Yen, B. K. H.; Stott, N. E.; Jensen, K. F.; Bawendi, M. G. A Continuous-Flow Microcapillary Reactor for the Preparation of a Size Series of CdSe Nanocrystals. *Adv. Mater.* **2003**, *15*, 1858–1862.
- (22) Lignos, I.; Protesescu, L.; Stavrakis, S.; Piveteau, L.; Speirs, M. J.; Loi, M. A.; Kovalenko, M. V.; deMello, A. J. Facile Droplet-based Microfluidic Synthesis of Monodisperse IV–VI Semiconductor Nanocrystals with Coupled In-Line NIR Fluorescence Detection. *Chem. Mater.* **2014**, *26*, 2975–2982.
- (23) Krishnadasan, S.; Brown, R. J. C.; deMello, A. J.; deMello, J. C. Intelligent routes to the controlled synthesis of nanoparticles. *Lab Chip* **2007**, *7*, 1434–1441.
- (24) Maceiczyk, R. M.; deMello, A. J. Fast and Reliable Metamodelling of Complex Reaction Spaces Using Universal Kriging. *J. Phys. Chem. C* **2014**, *118*, 20026–20033.
- (25) Nightingale, A. M.; Bannock, J. H.; Krishnadasan, S. H.; O’Mahony, F. T. F.; Haque, S. A.; Sloan, J.; Drury, C.; McIntyre, R.; deMello, J. C. Large-scale synthesis of nanocrystals in a multichannel droplet reactor. *J. Mater. Chem. A* **2013**, *1*, 4067–4076.
- (26) Nightingale, A. M.; deMello, J. C. Segmented Flow Reactors for Nanocrystal Synthesis. *Adv. Mater.* **2013**, *25*, 1813–1821.
- (27) Nightingale, A. M.; Krishnadasan, S. H.; Berhanu, D.; Niu, X.; Drury, C.; McIntyre, R.; Valsami-Jones, E.; deMello, J. C. A stable droplet reactor for high temperature nanocrystal synthesis. *Lab Chip* **2011**, *11*, 1221–1227.
- (28) Nightingale, A. M.; Phillips, T. W.; Bannock, J. H.; de Mello, J. C. Controlled multistep synthesis in a three-phase droplet reactor. *Nat. Commun.* **2014**, *5*, 1–8.
- (29) Chan, E. M.; Alivisatos, A. P.; Mathies, R. A. High-Temperature Microfluidic Synthesis of CdSe Nanocrystals in Nanoliter Droplets. *J. Am. Chem. Soc.* **2005**, *127*, 13854–13861.
- (30) Chan, E. M.; Mathies, R. A.; Alivisatos, A. P. Size-Controlled Growth of CdSe Nanocrystals in Microfluidic Reactors. *Nano Lett.* **2003**, *3*, 199–201.
- (31) Wang, H.; Li, X.; Uehara, M.; Yamaguchi, Y.; Nakamura, H.; Miyazaki, M.; Shimizu, H.; Maeda, H. Continuous synthesis of CdSe–ZnS composite nanoparticles in a microfluidic reactor. *Chem. Commun.* **2004**, *48*–49.
- (32) Wang, H.; Nakamura, H.; Uehara, M.; Yamaguchi, Y.; Miyazaki, M.; Maeda, H. Highly Luminescent CdSe/ZnS Nanocrystals Synthesized Using a Single-Molecular ZnS Source in a Microfluidic Reactor. *Adv. Funct. Mater.* **2005**, *15*, 603–608.
- (33) Marre, S.; Park, J.; Rempel, J.; Guan, J.; Bawendi, M. G.; Jensen, K. F. Supercritical Continuous-Microflow Synthesis of Narrow Size Distribution Quantum Dots. *Adv. Mater.* **2008**, *20*, 4830–4834.

- (34) Shestopalov, I.; Tice, J. D.; Ismagilov, R. F. Multi-step synthesis of nanoparticles performed on millisecond time scale in a microfluidic droplet-based system. *Lab Chip* **2004**, *4*, 316–321.
- (35) Zhang, L.; Niu, G.; Lu, N.; Wang, J.; Tong, L.; Wang, L.; Kim, M. J.; Xia, Y. Continuous and Scalable Production of Well-Controlled Noble-Metal Nanocrystals in Milliliter-Sized Droplet Reactors. *Nano Lett.* **2014**, *14*, 6626–6631.
- (36) Zhang, L.; Wang, Y.; Tong, L.; Xia, Y. Seed-Mediated Synthesis of Silver Nanocrystals with Controlled Sizes and Shapes in Droplet Microreactors Separated by Air. *Langmuir* **2013**, *29*, 15719–15725.
- (37) Zhang, L.; Wang, Y.; Tong, L.; Xia, Y. Synthesis of Colloidal Metal Nanocrystals in Droplet Reactors: The Pros and Cons of Interfacial Adsorption. *Nano Lett.* **2014**, *14*, 4189–4194.
- (38) Lignos, I.; Stavrakis, S.; Kilaj, A.; deMello, A. J. Millisecond-Timescale Monitoring of PbS Nanoparticle Nucleation and Growth Using Droplet-Based Microfluidics. *Small* **2015**, DOI: 10.1002/smll.201500119.
- (39) Abolhasani, M.; Oskooei, A.; Klinkova, A.; Kumacheva, E.; Gunther, A. Shaken, and stirred: oscillatory segmented flow for controlled size-evolution of colloidal nanomaterials. *Lab Chip* **2014**, *14*, 2309–2318.
- (40) Chakravarthy, V. S.; Ottino, J. M. Mixing of two viscous fluids in a rectangular cavity. *Chem. Eng. Sci.* **1996**, *51*, 3613–3622.
- (41) Chien, W.-L.; Rising, H.; Ottino, J. M. Laminar mixing and chaotic mixing in several cavity flows. *J. Fluid Mech.* **1986**, *170*, 355–377.
- (42) Abolhasani, M.; Bruno, N. C.; Jensen, K. F. Oscillatory three-phase flow reactor for studies of bi-phasic catalytic reactions. *Chem. Commun.* **2015**, *51*, 8916–8919.
- (43) Chen, D. L.; Gerdts, C. J.; Ismagilov, R. F. Using Microfluidics to Observe the Effect of Mixing on Nucleation of Protein Crystals. *J. Am. Chem. Soc.* **2005**, *127*, 9672–9673.
- (44) Song, H.; Bringer, M. R.; Tice, J. D.; Gerdts, C. J.; Ismagilov, R. F. Experimental test of scaling of mixing by chaotic advection in droplets moving through microfluidic channels. *Appl. Phys. Lett.* **2003**, *83*, 4664–4666.
- (45) Thulasidas, T. C.; Abraham, M. A.; Cerro, R. L. Bubble-train flow in capillaries of circular and square cross section. *Chem. Eng. Sci.* **1995**, *50*, 183–199.
- (46) Yu, W. W.; Qu, L.; Guo, W.; Peng, X. Experimental Determination of the Extinction Coefficient of CdTe, CdSe, and CdS Nanocrystals. *Chem. Mater.* **2003**, *15*, 2854–2860.
- (47) Qu, L.; Yu, W. W.; Peng, X. In Situ Observation of the Nucleation and Growth of CdSe Nanocrystals. *Nano Lett.* **2004**, *4*, 465–469.
- (48) Park, J.; Joo, J.; Kwon, S. G.; Jang, Y.; Hyeon, T. Synthesis of Monodisperse Spherical Nanocrystals. *Angew. Chem., Int. Ed.* **2007**, *46*, 4630–4660.
- (49) Harris, D. K.; Bawendi, M. G. Improved Precursor Chemistry for the Synthesis of III–V Quantum Dots. *J. Am. Chem. Soc.* **2012**, *134*, 20211–20213.
- (50) Allen, P. M.; Walker, B. J.; Bawendi, M. G. Mechanistic Insights into the Formation of InP Quantum Dots. *Angew. Chem., Int. Ed.* **2010**, *49*, 760–762.
- (51) Gary, D. C.; Glassy, B. A.; Cossairt, B. M. Investigation of Indium Phosphide Quantum Dot Nucleation and Growth Utilizing Triarylsilylphosphine Precursors. *Chem. Mater.* **2014**, *26*, 1734–1744.
- (52) Xie, R.; Battaglia, D.; Peng, X. Colloidal InP Nanocrystals as Efficient Emitters Covering Blue to Near-Infrared. *J. Am. Chem. Soc.* **2007**, *129*, 15432–15433.
- (53) Gielen, F.; van Vliet, L.; Koprowski, B. T.; Devenish, S. R. A.; Fischlechner, M.; Edel, J. B.; Niu, X.; deMello, A. J.; Hollfelder, F. A Fully Unsupervised Compartment-on-Demand Platform for Precise Nanoliter Assays of Time-Dependent Steady-State Enzyme Kinetics and Inhibition. *Anal. Chem.* **2013**, *85*, 4761–4769.